The influence of intraluminal thrombus on noninvasive abdominal aortic aneurysm wall distensibility measurement

Eleni Metaxa, Nikolaos Kontopodis, Vasileios Vavourakis, Konstantinos Tzirakis, Christos V. Ioannou & Yannis Papaharilaou

Medical & Biological Engineering & Computing

ISSN 0140-0118
Volume 53
Number 4

Med Biol Eng Comput (2015) 53:299-308
DOI 10.1007/s11517-014-1235-x

Springer

Med Biol Eng Comput (2015) 53:299–308
DOI 10.1007/s11517-014-1235-x

ORIGINAL ARTICLE

The influence of intraluminal thrombus on noninvasive abdominal aortic aneurysm wall distensibility measurement

Eleni Metaxa · Nikolaos Kontopodis · Vasileios Vavourakis · Konstantinos Tzirakis · Christos V. Ioannou · Yannis Papaharilaou

Received: 21 February 2014 / Accepted: 15 December 2014 / Published online: 30 December 2014

Abstract Abdominal aortic aneurysm wall distensibility can be estimated by measuring pulse pressure and the corresponding sac volume change, which can be obtained by measuring wall displacement. This approach, however, may introduce error if the role of thrombus in assisting the wall in bearing the pulse pressure loading is neglected. Our aim was to introduce a methodology for evaluating and potentially correcting this error in estimating distensibility. Electrocardiogram-gated computed tomography images of eleven patients were obtained, and the volume change between diastole and systole was measured. Using finite element procedures, we determined the equivalent pulse pressure loading that should be applied to the wall of a model where thrombus was digitally removed, to yield the same sac volumetric increase caused by applying the luminal pulse pressure to the model with thrombus. The equivalent instead of the measured pulse pressure was used in the distensibility expression. For a relative volumetric thrombus deposition (V_{ILT}) of 50 %, a 62 % distensibility underestimation resulted when thrombus role was neglected. A strong linear correlation was observed between distensibility underestimation and V_{ILT}. To assess the potential value of noninvasive wall distensibility measurement in rupture risk stratification, the role of thrombus on wall loading should be further investigated.

Keywords Arterial stiffness · Vascular biomechanics · 4D CT · Rupture risk · Young's modulus

E. Metaxa · K. Tzirakis · Y. Papaharilaou (✉)
Foundation for Research and Technology–Hellas, Institute of Applied and Computational Mathematics, Nikolaou Plastira 100, Vassilika Vouton, 70013 Heraklion, Crete, Greece
e-mail: yannisp@iacm.forth.gr

N. Kontopodis · C. V. Ioannou
Department of Vascular Surgery, Medical School, University of Crete, Heraklion, Crete, Greece

V. Vavourakis
Centre for Medical Image Computing, University College London, London WC1E 6BT, UK

1 Introduction

An important objective in cardiovascular research has been the accurate estimation of abdominal aortic aneurysm (AAA) rupture risk. According to the biomechanical approach, rupture occurs when strength of the degenerated aneurysmal wall can no longer withstand the stresses exerted on it due to intraluminal pulse pressure. Thus, if the wall strength, which changes as the aneurysm evolves [14], and stress distribution could be determined on a patient-specific basis, this information could be used to improve clinical management of AAA patients [5, 41].

Since wall strength cannot currently be measured in vivo, studies have attempted to correlate the latter with other wall mechanical properties such as distensibility [8]. Both strength and distensibility strongly depend on the composition of the arterial wall extracellular matrix. Wilson et al. [40] hypothesized that AAAs could be differentiated into two types: One where further AAA enlargement is accompanied by increased deposition of collagen fibers to sustain the internal forces, and would show an increase in wall stiffness, and another where the AAA fails to lay down and remodel collagen, and would be weaker and more distensible. Indeed, AAAs progressing to rupture tended to be more distensible compared to those that did not rupture during follow-up [40]. Furthermore, direct ex vivo measurements of aortic stiffness also revealed that AAAs being less stiff were also weaker [8]. Moreover, regarding large

aneurysms, wall strength was related to wall thickness or stiffness [8].

In light of wall distensibility association with wall strength, studies evaluated its potential role in AAA rupture risk estimation by recording the aortic wall motion during the cardiac cycle using 4D imaging. Distensibility of a material is generally defined as the deformation divided by the loading, and for arteries, it is commonly expressed as the fractional increase in volume divided by the pressure pulse:

$$D = \frac{\Delta V}{V_0 \cdot \Delta P} \quad (1)$$

While arterial distensibility has been extensively investigated in clinical research (i.e., hypertension), AAA wall distensibility determination is not straight forward due to intraluminal thrombus (ILT) presence (in more than 70 % of AAAs). ILT affects wall loading which thus deviates from luminal pulse pressure. Many studies have determined AAA wall compliance using aortic pulse pressure, but it has been questioned if the estimates of distensibility obtained reflected the extent and distribution of thrombus [20].

The effect of ILT on wall loading remains controversial [39]. Two important factors in determining the presence or extent of ILT's potential stress shielding effect are the attachment of thrombus to the underlying wall and the degree of ILT porosity and compressibility. In vivo [29] and in vitro [16] studies have shown that the pore pressure in ILT approximately equals blood pressure and suggested that ILT does not reduce wall stresses [29]. On the other hand, computational [9, 19, 24, 25, 38] and experimental studies [33] have demonstrated that ILT considerably lowers wall stress and strain. These seemingly opposite findings can both be true if ILT is indeed a structural component with typical solid mechanical properties [3, 7, 10, 35, 37], but with interconnected cavities and pores filled with fluid [6, 11] that is fully attached to the wall; the entire luminal pressure is transferred through the ILT pores to the vessel wall, while the fibrous network of ILT, which adheres to the wall, helps the wall carry the pulse pressure load, thus reducing wall stress and strain [26, 33]. Indeed, Meyer et al. [22] have recently shown that the thrombus can have a stress-reducing role even if it does not directly reduce pressurization of the wall if ILT is assumed fully attached to the wall. Since ILT may affect wall stress, it is important to consider this when estimating wall distensibility.

We have previously measured the fractional expansion of the AAA wall and luminal surface from diastole to systole in AAA patients and calculated the wall-ILT composite distensibility for which loading is directly represented by luminal pulse pressure [18]. Here, we seek to assess the potential error in wall distensibility calculation when the effect of ILT on wall loading is ignored and propose a methodology that could be applied to address this issue.

2 Methods

2.1 Study population

Eleven consecutive patients with AAA were included in this study, which was approved by the local institutional ethics committee, and all subjects gave informed consent. Mean age was 71.7 years ranging from 59 to 82 years. The male:female ratio was 10:1. Maximum diameter of the studied AAAs ranged from 32 mm to 68 mm with an average of 50 mm.

2.2 Data acquisition

All patients underwent multi-detector electrocardiogram-gated (ECG-gated) computed tomography (CT) scans. Image acquisition was performed with a Somatom definition flash, dual-source–dual-energy CT scanner (Siemens, Erlangen, Germany), before and after contrast media administration with retrospective ECG-gated spiral acquisition. Non-ionic contrast media were used, and the total effective dose was 5.5 mSv at 80 bpm. Slice thickness was 0.625 mm and image matrix size 512 × 512. The temporal resolution was 83 ms and in-plane spatial resolution 0.33 mm. Two ECG-gated series of axial images were reconstructed at peak systole and end diastole during the R–R interval. The brachial pressure measurements were obtained.

2.3 Image segmentation and 3D surface reconstruction

Segmentation and 3D surface reconstruction of the aortic wall and lumen were performed manually using the software ITK-SNAP [42]. Briefly, outlines of the outer surface of the wall and the luminal surface of the aorta were manually obtained slice by slice, and the 3D surfaces were reconstructed from the stack of contours. The segmentation included the visceral segment of the abdominal aorta to obtain information of a seemingly healthy vessel, to approximately 4 cm below the aortic bifurcation including a part of the iliac arteries. The surfaces were smoothed using the Taubin volume-preserving smoothing algorithm [32], which is implemented in the vascular modeling toolkit (VMTK) software [2]. A passband of 0.01 and 80 iterations was used, that removed surface noise without changing the AAA sac volume more than 0.2 %.

2.4 Evaluation of wall loading

For the estimation of wall loading reduction in the presence of ILT, finite element analysis (FEA) was used. For

the purpose of obtaining a relationship between wall loading reduction and the volumetric percentage of ILT in the sac, V_{ILT}, five AAA cases (out of the 11) that presented a wide range of ILT accumulation were selected, and their end diastole series were used.

2.4.1 Geometrical AAA model construction

Due to lack of information on wall thickness distribution, we assumed an uniform thickness of 2 mm. The wall surface reconstructed from the CT images was used to generate two new surfaces: an "internal" wall surface by inward offsetting the initial surface by 1 mm, and an "external" wall surface by outward offsetting the initial surface by 1 mm.

2.4.2 Mesh generation

The 3D mesh was generated using ICEM CFD v.12.0.1 (ANSYS Inc., Berkeley, CA, USA). The mesh consisted of linear tetrahedral elements. Mesh independency tests were carried out: An AAA geometry was discretized with 0.2, 0.3, and 0.4 million elements (ME), and the AAA volume increase (the parameter measured in this study) was computed with FEA applying the measured pressure loading for each case (methodology described below). The difference in volume increase was less than 1 % between the three meshes used, and we thus considered the solution for the 0.3 ME case mesh independent. Thus, the solid mesh in each AAA model had approximately 0.3 ME when ILT was abundant, and approximately 0.17 ME when ILT was minimal or absent. The average maximum element edge length was 1.5 mm, while the mesh density was 2.4–2.6 elements/mm^3.

2.4.3 Finite element analysis solver

As reported in [21], it is necessary for accurate AAA biomechanical modeling to recover the zero-pressure state configuration of the vessel wall, in order to improve wall distensibility estimation. A similar observation was made in the FSI analysis presented in [36], where both vessel wall deformation and blood flow characteristics were affected when the measured and not the zero-pressure state geometry of a carotid bifurcation was used in the FSI analysis. Along these lines, we utilized an inverse finite deformation FEA, originally proposed by Govindjee and Mihalic [12], to recover the zero-pressure state configuration of the vessel wall with the ILT. In this regard, we developed an in-house finite element solver [36] that was based on the open-source C++ library libMesh [17].

Moreover, a recent computational study integrating a poroelastic description of ILT has shown that wall stress is insensitive to ILT permeability, and that similar wall stress estimates where obtained from both poroelastic and single-phase ILT descriptions [26]. Following this observation, a single-phase ILT material model is assumed here.

Specifically, the aortic wall and the ILT were assumed to be isotropic, near-incompressible, hyperelastic materials. The adopted strain–energy function expressions for the wall and the ILT were the following, respectively:

$$W_{\text{wall}} = \alpha(I-3) + \beta(\mathrm{I}-3)^2 + \frac{k}{2}(\log J)^2,$$

$$W_{\text{ILT}} = c_1(\mathrm{II}-3) + c_2(\mathrm{II}-3)^2 + \frac{k}{2}(\log J)^2$$

where $\alpha = 0.174$ MPa and $\beta = 1.88$ MPa [27], $c_1 = c_2 = 0.026$ MPa [37], I, II the first and second invariant of the right Green–Cauchy deformation tensor C, J the deformation gradient determinant, and $k = 10^3$ MPa a penalty parameter for enforcing the near-incompressible behavior of blood vessel wall and ILT tissues.

2.4.4 Wall loading estimation

In order to estimate the wall loading in the presence of ILT, we implemented the following methodology presented in Fig. 1. First, for each reconstructed AAA model, we applied inverse finite element analysis to recover its zero-pressure state geometric configuration. Next, forward finite element simulations were carried out in order to obtain the sac geometry at diastole (V_D) and systole (V_S), by applying diastolic (P_D) and systolic pressure (P_S) loading, respectively, on the luminal surface of ILT. We computed the sac volumes, as described in the next paragraph. Subsequently, the ILT (gray region) was digitally removed from the zero-pressure state configuration of the AAA model, and the sac was filled only by the lumen (orange region). The equivalent wall pressure was determined numerically at diastole ($\tilde{P}_D$) and systole ($\tilde{P}_S$) by trial-and-error and keeping constant the material parameters and changing the applied luminary pressure, so that when applied to the AAA wall yields V_D and V_S, respectively. For this convergence study, when the difference between the volume achieved and the desired volume was less than 0.1 %, linear interpolation was used to obtain the equivalent pressure.

The equivalent pulse pressure ($\Delta\tilde{P} = \tilde{P}_S - \tilde{P}_D$) is then used in Eq. (1) for the calculation of corrected wall distensibility ($\tilde{D}$). Although our region of interest was the AAA sac, the computational domain of the artery also included part of the neck region and the iliac arteries.

The distensibility error, d_{error}, when ignoring the ILT effect on wall loading, was calculated based on the $\Delta\tilde{P}$, as:

$$d_{\text{error}} = \frac{\tilde{D}-D}{\tilde{D}} = \frac{\frac{\Delta V}{V_0\cdot\Delta\tilde{P}} - \frac{\Delta V}{V_0\cdot\Delta P}}{\frac{\Delta V}{V_0\cdot\Delta\tilde{P}}} = \frac{\Delta P - \Delta\tilde{P}}{\Delta P}$$

$$\text{or } d_{\text{error}} = 1 - \frac{\Delta\tilde{P}}{\Delta P} \tag{2}$$

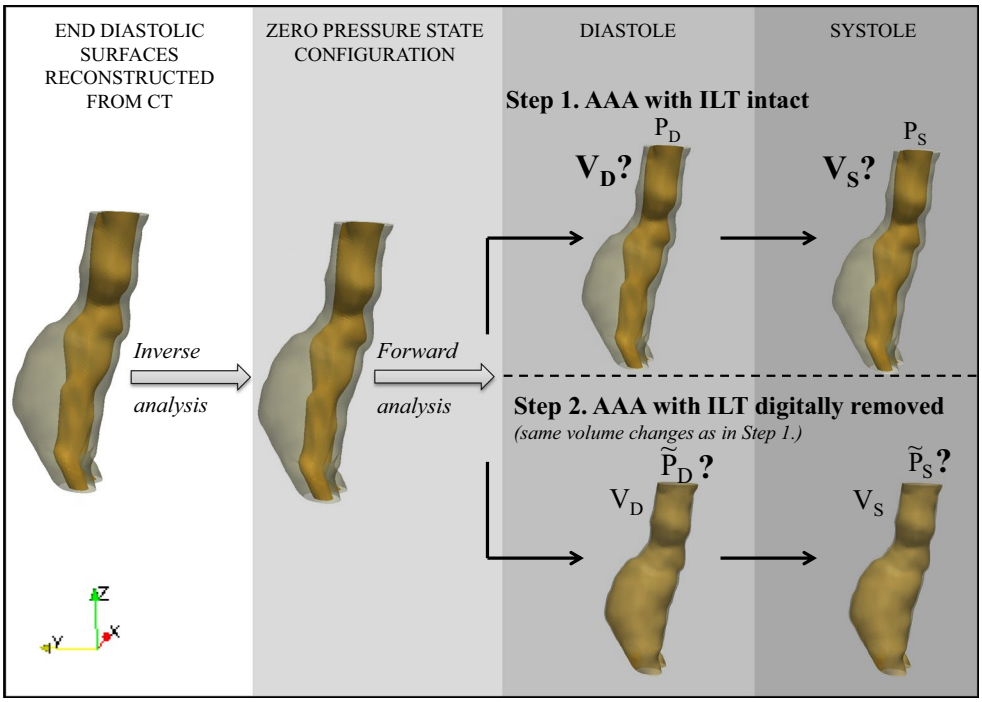

Fig. 1 Methodology for determining the equivalent wall pressures. Starting from the end diastolic geometry reconstructed from CT images, the zero-pressure state configuration was computed. *Step 1* Applying diastolic (P_D) and then systolic pressure (P_S) on the lumen wall, the AAA volume at diastole (V_D) and systole (V_S) was computed. *Step 2* The ILT was digitally removed from the zero-pressure state AAA model, and the diastolic ($\tilde{P}_D$) and systolic pressure ($\tilde{P}_S$) were computed which yield the AAA volume increase computed in Step 1 ($\Delta V = V_S - V_D$). The CT scanner coordinate system embedded in the acquired images is used for AAA orientation. The positive *Y*-axis here points toward the patient anterior side

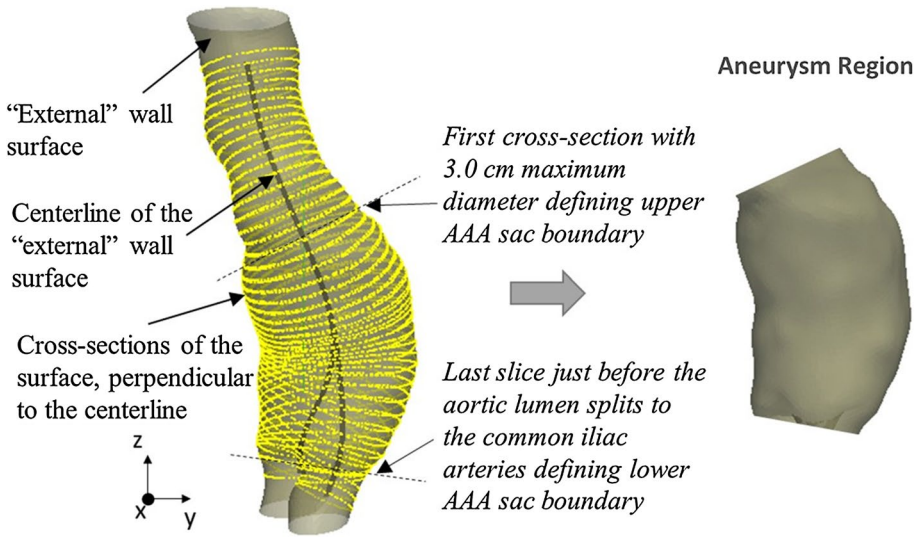

Fig. 2 Aneurysm region determination. Cross sections of "external" wall surface at 0.1 cm intervals (here slices every 0.3 cm are shown) normal to the centerline are extracted. The AAA region considered was defined between the most proximal cross section with $D > 3$ cm and the most distal cross section before the split of the aortic lumen to the common iliac arteries

To alleviate the need for FEA to obtain$\Delta\tilde{P}$, a correlation between distensibility error and volumetric percentage of ILT in the sac was sought: $d_{\text{error}} = f(V_{\text{ILT}})$.

2.4.5 AAA volume determination

For the AAA sac volume calculation, VMTK was first used to extract the region of interest. Specifically, the centerline of the "external" wall surface was computed, and cross sections normal to the centerline were obtained at 0.1-mm intervals (Fig. 2). The boundaries of the AAA sac were defined as the most proximal cross section with 3.0 cm maximum diameter of the "external" wall surface to the last slice just before the aortic lumen splits to the common iliac arteries, or to the most distal aortic cross section with 3.0 cm maximum diameter. After cropping the AAA region, the volumes of AAA sac at diastole and systole were calculated with the open-source software GNU Triangulated Surface Library 0.7.6. The V_{ILT} was calculated based on the fraction of thrombus volume in the aneurysm volume using the following equation:

Table 1 Distensibility error (d_{error}) for five AAA cases

Data for V_{ILT} foretell a relationship between d_{error} and the amount of ILT accumulation

Case #	Luminal pressure (mmHg)		Equivalent wall pressure (mmHg)		Pulse pressure (mmHg)		d_{error} (%)	V_{ILT} (%)
	Diastole P_D	Systole P_S	Diastole $\tilde{P}_D$	Systole $\tilde{P}_S$	Luminal ΔP	Wall $\Delta\tilde{P}$		
2	80	150	10	18	70	8	88	82
4	80	130	15	23	50	8	82	73
5	77	123	21	34	46	13	72	71
6	80	120	28	44	40	18	62	64
10	108	195	58	111	87	53	40	50

$$V_{ILT} = \frac{V_{Wall} - V_{Lumen}}{V_{Wall}}$$

where V_{Wall} and V_{Lumen} are the volumes enclosed by the AAA inner wall surface and AAA lumen surface at diastole, respectively.

2.5 Application: image-based wall distensibility estimation in a patient cohort

Having obtained a correlation between d_{error} and V_{ILT}, we estimated AAA wall distensibility in 11 patients without using FEA. Wall distensibility was evaluated provided the ECG-gated acquired wall displacement between diastole and systole, the aortic pulse pressure, and V_{ILT}, using the expression:

$$\tilde{D} = \frac{\Delta V}{V_0 \cdot \Delta P} \Big/ (1 - d_{error}) = \frac{\Delta V}{V_0 \cdot \Delta P} \Big/ (1 - f(V_{ILT})). \quad (3)$$

Specifically, for the determination of the $\Delta V/V_0$ ratio, the CT series at peak systole and end diastole were used, as described elsewhere [18]. Briefly, using VMTK as described above, we calculated the AAA volume enclosed by the outer wall at diastole and the luminal volume at diastole and systole. Assuming ILT to be incompressible, the volume increase in the lumen equals that of the AAA, which divided by the AAA volume yields the AAA fractional volumetric increase ($\Delta V/V_0$). The maximum diameter, d_{max}, was recorded on the orthogonal slices for each AAA at the diastolic phase.

From the brachial pressure measurements, the abdominal aortic blood pressure at diastole and systole was estimated based on the correction proposed in [34], where the brachial systolic pressure was found to underestimate the aortic pressure by 5 % and the brachial diastolic pressure to overestimate the aortic pressure by 12 %.

For the wall displacement estimation, a primary source of uncertainty is the image segmentation process, which has previously been evaluated by segmenting two AAA cases by two blinded-independent observers [18]. Using these two segmentations, we obtained the interobserver mean difference in the fractional volumetric increase in AAA ($\Delta V/V_0$) required for the distensibility calculation. To obtain a measure of uncertainty in distensibility calculation (D, $\tilde{D}$) for each AAA, the interobserver mean difference in $\Delta V/V_0$ was used in Eq. 1 and 3, respectively.

For the purpose of comparing our distensibility results with other studies, the Young's modulus, before correction (E) and after correction ($\tilde{E}$), was also calculated for all AAA cases based on the equations:

$$E = \frac{R_{\alpha\nu}(1-\nu^2)}{h \cdot D} \text{ and } \tilde{E} = \frac{R_{\alpha\nu}(1-\nu^2)}{h \cdot \tilde{D}},$$

where $R_{\alpha\nu}$ represents the radius of the cylinder that has a volume equal to the AAA sac volume at diastole and length equal to the AAA length (centerline length), ν is Poisson's ration (0.5), and h is the wall thickness (2 mm).

Regression analysis was conducted in Excel (Microsoft, Redmond, WA, USA). A linear fit and its R^2 value between d_{error} and V_{ILT} were obtained. The correlations between D and $\tilde{D}$ with d_{max} were evaluated based on the R^2 of a linear curve fit.

3 Results

3.1 Distensibility error when ILT effect on wall loading is neglected

The results of applying the methodology presented in Fig. 1 for determining the equivalent wall pressures $\tilde{P}_D$ and $\tilde{P}_S$ in diastole and systole, respectively, and the associated distensibility error for five AAA cases with V_{ILT} in the range of 50–82 % is presented in Table 1.

Of note is that for all cases considered, computed values of $\tilde{P}_D$ and $\tilde{P}_S$ were substantially lower than luminal pressures, P_D and P_S, respectively. Interestingly, the computed equivalent wall pressure pulse $\Delta\tilde{P}$ was also markedly reduced as compared to the luminal pressure pulse ΔP for all cases considered. This, as expected based on the definition of d_{error}, suggests large errors in distensibility

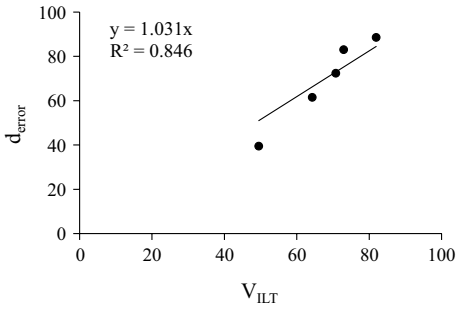

Fig. 3 Linear fit between d_{error} and V_{ILT}

estimation when ILT role is neglected. Note that d_{error} may become very high (>80 %) in AAA cases where relative ILT accumulation in the sac is >72 %. Based on the values of V_{ILT} presented in Table 1, a positive correlation with d_{error} was apparent. In Fig. 3, V_{ILT} was plotted against d_{error}, and a good linear fit ($R^2 = 0.846$) was found described by the following expression:

$$d_{error} = 1.031 \cdot V_{ILT} \quad (4)$$

3.2 Application: image-based wall distensibility estimation in a patient cohort

Table 2 presents, for our AAA patient cohort, errors in distensibility estimation based on Eq. 4 along with distensibility estimates for both healthy aortic and AAA wall sections based on Eq. 1. Corrected distensibility values for AAA wall based on Eq. 3 are also presented, as well as Young's modulus before and after correction. Of note is that in all cases, $\tilde{D}$ was higher compared to D. Additionally, in contrast to most large AAAs ($d_{max} > 5$ cm, e.g., cases 1, 4, 5, 6), most small AAAs ($d_{max} < 5$ cm, e.g., cases 7, 8, 9, 10, 11) presented a stiffer wall compared to that of healthy upper aortic segment (AAA $\tilde{D}$ < Healthy D). Two cases, however, presented an opposite trend. In case 2 ($d_{max} = 4.7$ cm), AAA wall was more distensible compared to its upper healthy segment, while in case 3 ($d_{max} = 5.2$ cm), AAA wall was less distensible compared to their upper healthy segment. It should be noted that the absolute values of AAA wall distensibility among the two cases were similar, but there was a difference in the distensibility of their upper aortic segment.

The mean interobserver difference in $\Delta V/V_0$ was 0.0004, which is one order of magnitude smaller than the measured $\Delta V/V_0$ of AAA sac.

Figure 4 shows correlation of wall distensibility estimate with maximum diameter when ILT effect is either excluded (Fig. 4a) or included (Fig. 4b) in the analysis.

As shown in Fig. 3a, no correlation ($R^2 = 0.01$) was found between D (Eq. 1) and d_{max}. However, $\tilde{D}$ (Eq. 3) presented a positive correlation ($R^2 = 0.568$) with d_{max} (Fig. 4b).

4 Discussion

With the advances in imaging techniques, wall distensibility estimation is gaining increasing interest for its potential use in noninvasive determination of AAA wall mechanical properties, toward a more sensitive, patient-specific rupture

Table 2 Accounting for ILT mechanical effect in AAA wall distensibility (AAA $\tilde{D}$), based on the distensibility estimation error (d_{error}) for all AAA cases

Case #	d_{max} (mm)	$\Delta V/V_0$ healthy	ΔP (mmHg)	Healthy D (MPa^{-1})	$\Delta V/V_0$ AAA	AAA D (MPa^{-1})	E (MPa)	V_{ILT} (%)	d_{error} (%)	AAA $\tilde{D}$ (MPa^{-1})	$\tilde{E}$ (MPa)
1	68	0.025	67.0	2.83	0.007	0.74	14.96	76	78	3.42	3.24
2	47	0.013	86.5	1.13	0.006	0.49	15.10	82	85	3.17	3.27
3	52	0.055	71.5	5.74	0.028	2.90	2.60	15	15	3.43	2.20
4	65	0.010	50.0	1.47	0.010	1.50	6.36	73	75	6.06	1.57
5	53	0.027	60.7	3.29	0.008	0.96	7.71	71	73	3.58	2.07
6[a]	58	0.009	54.9	1.17	0.013	1.77	4.42	64	66	5.20	1.50
7	44	0.041	67.0	4.61	0.008	0.92	7.50	55	57	2.12	3.25
8	40	0.030	44.4	5.13	0.017	2.81	2.35	19	20	3.49	1.89
9	32	0.043	63.9	5.08	0.005	0.53	9.54	19	20	0.66	7.67
10	49	0.041	108.8	2.80	0.012	0.82	8.77	50	52	1.69	4.25
11	41	0.016	54.9	2.13	0.004	0.57	10.96	22	23	0.74	8.48

Distensibility calculation of healthy (Healthy D) and AAA (AAA D) wall using Eq. 1, where fractional volumetric increase ($\Delta V/V_0$) and aortic pulse pressure (ΔP) are used. For corrected AAA distensibility (AAA $\tilde{D}$), V_{ILT} is also taken into account (Eq. 3). Young's modulus before (E) and after correction ($\tilde{E}$) is also presented. Maximum diameter (d_{max}) for each AAA is listed

[a] Brachial pressure was unavailable, and a physiological pulse pressure was used

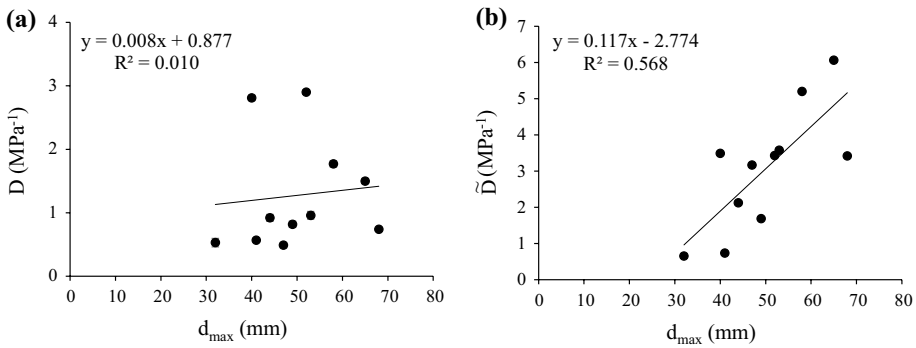

Fig. 4 Correlation of wall distensibility with maximum diameter. **a** Excluding and **b** including ILT mechanical effect in the analysis. *Error bars* (visible at the boundaries of *data symbols*) are calculated based on the mean interobserver difference in the fractional volumetric increase

Table 3 Comparison of biomechanical properties between our results and others

	Our study		Others	
D (MPa^{-1})	0.53–2.9		0.5–3 [34]	
	Before correction	After correction	In vivo estimation	Ex vivo measurements
Young's modulus (MPa)	2.35–15.10	1.50–8.48	5.50–12.90 [34]	0.30–9.50 [8]

risk assessment. However, while the wall displacement can be measured exploiting 4D imaging techniques, the wall loading in the presence of ILT, required for the distensibility calculation, cannot be obtained directly from noninvasive measurements. We showed that a marked error in wall distensibility estimation may occur if the effect of ILT on wall loading is neglected.

Interestingly, a positive correlation between the distensibility error and the relative ILT sac volume was found. While other factors, such as AAA geometry and ILT distribution, are also expected to affect the mean wall loading, and subsequently the computed equivalent wall pressure, the relative ILT sac volume had a relatively strong correlation with the distensibility error that appears, in these cases at least, to be one of the main determinants.

The correction in distensibility not only increased the distensibility values of each AAA but also changed the relationship between distensibility and AAA size. While large AAAs initially had shown a "stiff behavior" based on their wall displacement data, this was mainly attributed to the reduced wall loading due to ILT presence. The error was less in smaller AAAs (d_{max} < 50 mm) due to lower ILT deposition. After the correction (Fig. 3b), the distensibility seemed to increase with size, but the correlation was not so strong: Not all large AAAs (>50 mm) presented increased distensibility, while there was one AAA with d_{max} < 50 mm (case 2) that was more distensible than the upper aortic wall. Could this AAA be of high rupture risk? A large follow-up study could show whether distensibility is associated with high rupture risk potential and, thus, be incorporated in a rupture risk assessment model.

Our results appear in agreement with previous studies. Specifically, we found that in most of the small AAAs, the wall appears to be stiffer than the upper aortic segment, which agrees with previous studies [13, 23, 30]. However, some large AAAs in our study appeared to be more distensible compared to the upper aortic segment. Molacek et al. [23], who although did not account for the effect of ILT on wall loading in their analysis, also found AAA distensibility values that either reached or even exceeded the values of the upper healthy aorta. Wilson's et al. observed that AAAs that did not become stiffer, or became more distensible during their evolution were at a particularly high risk of rupture [40]. Should we assume that the larger AAAs in our study cohort are in a greater risk of rupture, it would be reasonable for them to appear more distensible.

In order to examine the physiological relevance of the distensibility values obtained, we compared them before correction with previous in vivo studies that neglected the effect of thrombus on wall loading and the distensibility values after correction with previously reported results on mechanical testing of AAA tissues (Table 3). Our results before correction agree with those of van't Veer et al. [34], that similarly used the volumetric increase and the aortic pulse pressure for the distensibility estimation. However, while this study [34] shows good agreement with previous in vivo estimations of AAA distensibility, they measured a 3–4 times higher AAA wall Young's modulus compared to previously reported ex vivo mechanical testing of tangential moduli of AAA specimens [8]. They suggest that a difference in wall thickness between the two studies might be the reason for such a difference, but based on the present study, this difference may also be due to the effect of ILT on wall loading, which they have ignored. We also measured Young's modulus for all cases. It is interesting to note that for case 1 and case 2 (which presented the largest V_{ILT} and subsequently the largest increase in distensibility after correction), it was found 14.96 and 15.1 MPa, respectively, before distensibility correction. Although these values fall outside the range obtained by ex vivo testing [8], the

corrected value of 3.24 and 3.27 MPa, respectively, fall inside that range. Therefore, the obtained distensibility values after correction appear to better represent the true physical situation.

It is worth commenting that a Young's modulus-based description of the mechanical behavior of an artery is rather simplifying as AAA wall has been shown to exhibit hyperelastic material behavior [27]. The Young's modulus found here describes the artery's elasticity at the applied range of pressures only.

In general, there are several methods applied to estimate distensibility. We selected to measure distensibility from volume changes rather than changes in cross section (or diameter) at the site of maximum expansion, since the degenerative changes affect the entire AAA, and measuring the overall behavior seems more realistic [34].

Another concern when estimating AAA wall distensibility is the region selected to measure volume changes. This has previously been defined as the region spanning from just distal to the lowest renal artery to the most proximal to the aortic bifurcation [34]. However, this measurement could be problematic as this may also include a potentially healthy segment, which is expected to have different mechanical properties. In this study, the AAA and healthy segment regions were considered separately in the volume change calculation for the distensibility estimations.

Several studies have shown that the presence of thrombus reduces the wall stresses. Speelman et al. [31] have shown a 37 % mean reduction in peak wall stress (PWS) in a case that presented a mean relative ILT volume of 55 %. We also found that the equivalent wall pressure is substantially reduced compared to the luminal pressure. For example, in case 5, whose relative ILT volume was similar to the mean value in [31], there was a 72 % reduction between luminal (123 mmHg) and equivalent wall (34 mmHg) pressure at systole. At first, such a reduction would seem to be unrealistically and two times higher compared to [31]. However, the difference is mainly due to the fact that PWS is a local value that may not be affected as much from the total ILT volume in the sac, as it is greatly affected by the local ILT thickness and the wall surface curvature. On the other hand, the equivalent wall pressure represents a mean loading value affected by the total volume of ILT. To prove our point, we calculated the PWS and the mean wall stress for case 5, when the systolic pressure, P_S, was applied at the zero-pressure state configuration, in the presence and the absence of thrombus. The PWS presented a 39 % reduction when ILT was added to the model (similarly to the observations made in [31]), and a 63 % reduction in the mean wall stress (similarly to the luminal and equivalent pressure reduction). This reduction is a result of a stress shielding effect that the ILT has with the present commonly used material properties and FEA modeling. Our FEA modeling, therefore, does not result in a wall stress reduction that is substantially different from previously reported stress drop in the presence of ILT.

4.1 Limitations

A limitation of the FEA model is the uniform wall thickness assumption. While it is known that wall thickness varies within and between patients [15] and may affect the resulting wall stress estimates, and there is currently no noninvasive technique available to measure it accurately. However, if the spatial average of our patient-specific variable wall thickness was known and used, the results would probably not change significantly, as far as the spatial maxima of the first principal stress, strain, strain-energy density, and displacement [28].

Another limitation is the material model for ILT used in the FEA which may not accurately represent the actual mechanical effect of ILT on wall loading. The hyperelastic material model used for ILT is a two-parameter, near-incompressible, polynomial constitutive model that has been developed based on uniaxial tensile tests on AAA specimens, showing a good fit to the experimental data [27]. However, more recent studies, where the material properties of thrombus were re-evaluated with compression and shear experiments, indicated that ILT has a lower elastic modulus than that determined previously by uniaxial or biaxial tensile tests [3, 35], and it comprises of three different layers [3]. Therefore, while the poroelastic character of ILT [1, 4] seems to not affect the wall stress [26], a multilayered, nonhomogenous model of ILT may be needed before an accurate determination of ILT mechanical effect can be computed. The results presented here are, therefore, limited to the assumption of the ILT material model used and hence show the marked effect that the ILT may have in the noninvasive distensibility estimation, and highlight that in vivo estimation of AAA wall distensibility can probably not be performed before the ILT mechanical effect is accurately characterized. Furthermore, the present study proposes a methodology of distensibility correction that can potentially be easily adjusted when a more accurate ILT mechanical modeling is developed.

5 Conclusions

This study investigated the role of ILT on AAA wall loading in the context of wall distensibility noninvasive estimation. We showed that the presence of intraluminal thrombus could have a marked impact, bound to the material model assumptions, leading to AAA wall distensibility underestimation. Applying an isotropic hyperelastic material model for ILT, we found, for a typical V_{ILT} of 50 %, a distensibility

underestimation of ~50 %. To assess the potential value of noninvasive wall distensibility measurement in AAA rupture risk stratification, further investigation on the role of ILT on AAA wall loading is warranted.

Acknowledgments The research project is financially supported by the Action "Supporting Postdoctoral Researchers", co-financed by the European Social Fund (ESF) and the Greek State.

References

1. Adolph R, Vorp DA, Steed DL, Webster MW, Kameneva MV, Watkins SC (1997) Cellular content and permeability of intraluminal thrombus in abdominal aortic aneurysm. J Vasc Surg 25:916–926
2. Antiga L, Piccinelli M, Botti L, Ene-Iordache B, Remuzzi A, Steinman DA (2008) An image-based modeling framework for patient-specific computational hemodynamics. Med Biol Eng Comput 46:1097–1112
3. Ashton JH, Vande Geest JP, Simon BR, Haskett DG (2009) Compressive mechanical properties of the intraluminal thrombus in abdominal aortic aneurysms and fibrin-based thrombus mimics. J Biomech 42:197–201
4. Boschetti F, Di Martino EM, Giota G (2007) A poroviscoelastic model of intraluminal thrombus from abdominal aortic aneurysms. In: 2007 Summer bioengineering conference, Keystone CO
5. Breeuwer M, de Putter S, Kose U, Speelman L, Visser K, Gerritsen F, Hoogeveen R, Krams R, van den Bosch H, Buth J, Gunther T, Wolters B, van Dam E, van de Vosse F (2008) Towards patient-specific risk assessment of abdominal aortic aneurysm. Med Biol Eng Comput 46:1085–1095
6. Collet JP, Shuman H, Ledger RE, Lee S, Weisel JW (2005) The elasticity of an individual fibrin fiber in a clot. Proc Natl Acad Sci U S A 102:9133–9137
7. Di Martino E, Mantero S, Inzoli F, Melissano G, Astore D, Chiesa R, Fumero R (1998) Biomechanics of abdominal aortic aneurysm in the presence of endoluminal thrombus: experimental characterisation and structural static computational analysis. Eur J Vasc Endovasc Surg 15:290–299
8. Di Martino ES, Bohra A, Van de Geest JP, Gupta N, Makaroun MS, Vorp DA (2006) Biomechanical properties of ruptured versus electively repaired abdominal aortic aneurysm wall tissue. J Vasc Surg 43:570–576 (discussion 576)
9. Doyle BJ, Callanan A, McGloughlin TM (2007) A comparison of modelling techniques for computing wall stress in abdominal aortic aneurysms. Biomed Eng Online 6:38
10. Gasser TC, Gorgulu G, Folkesson M, Swedenborg J (2008) Failure properties of intraluminal thrombus in abdominal aortic aneurysm under static and pulsating mechanical loads. J Vasc Surg 48:179–188
11. Gasser TC, Martufi G, Auer M, Folkesson M, Swedenborg J (2010) Micromechanical characterization of intra-luminal thrombus tissue from abdominal aortic aneurysms. Ann Biomed Eng 38:371–379
12. Govindjee S, Mihalic P (1998) Computational methods for inverse deformations in quasi-incompressible finite elasticity. Int J Numer Meth Eng 43:821–838
13. He CM, Roach MR (1994) The composition and mechanical properties of abdominal aortic aneurysms. J Vasc Surg 20:6–13
14. Helderman F, Manoch IJ, Breeuwer M, Kose U, Schouten O, van Sambeek MR, Poldermans D, Pattynama PT, Wisselink W, van der Steen AF, Krams R (2008) A numerical model to predict abdominal aortic aneurysm expansion based on local wall stress and stiffness. Med Biol Eng Comput 46:1121–1127
15. Hellenthal FA, Geenen IL, Teijink JA, Heeneman S, Schurink GW (2009) Histological features of human abdominal aortic aneurysm are not related to clinical characteristics. Cardiovasc Pathol 18:286–293
16. Hinnen JW, Koning OH, Visser MJ, Van Bockel HJ (2005) Effect of intraluminal thrombus on pressure transmission in the abdominal aortic aneurysm. J Vasc Surg 42:1176–1182
17. Kirk B, Peterson J, Stogner R, Carey G (2006) libMesh: a C++ library for parallel adaptive mesh refinement/coarsening simulations. Eng with Comput 22:237–254
18. Kontopodis N, Metaxa E, Pagonidis K, Ioannou C, Papaharilaou Y (2013) Deformation and distensibility distribution along the abdominal aorta in the presence of aneurysmal dilatation. J Cardiovasc Surg (Torino) (in press)
19. Li ZY, Tang TY, Soh E, See TC, Gillard JH (2008) Impact of calcification and intraluminal thrombus on the computed wall stresses of abdominal aortic aneurysm. J Vasc Surg 47:928–935
20. MacSweeney ST (1999) Mechanical properties of abdominal aortic aneurysm and prediction of risk of rupture. Cardiovasc Surg 7:158–159
21. Merkx MA, van't Veer M, Speelman L, Breeuwer M, Buth J, van de Vosse FN (2009) Importance of initial stress for abdominal aortic aneurysm wall motion: dynamic MRI validated finite element analysis. J Biomech 42:2369–2373
22. Meyer CA, Guivier-Curien C, Moore JE Jr (2010) Trans-thrombus blood pressure effects in abdominal aortic aneurysms. J Biomech Eng 132:071005
23. Molacek J, Baxa J, Houdek K, Treska V, Ferda J (2011) Assessment of abdominal aortic aneurysm wall distensibility with electrocardiography-gated computed tomography. Ann Vasc Surg 25:1036–1042
24. Molony DS, Callanan A, Kavanagh EG, Walsh MT, McGloughlin TM (2009) Fluid-structure interaction of a patient-specific abdominal aortic aneurysm treated with an endovascular stent-graft. Biomed Eng Online 8:24
25. Mower WR, Quinones WJ, Gambhir SS (1997) Effect of intraluminal thrombus on abdominal aortic aneurysm wall stress. J Vasc Surg 26:602–608
26. Polzer S, Gasser TC, Markert B, Bursa J, Skacel P (2012) Impact of poroelasticity of intraluminal thrombus on wall stress of abdominal aortic aneurysms. Biomed Eng Online 11:62
27. Raghavan ML, Vorp DA (2000) Toward a biomechanical tool to evaluate rupture potential of abdominal aortic aneurysm: identification of a finite strain constitutive model and evaluation of its applicability. J Biomech 33:475–482
28. Raut SS, Jana A, De Oliveira V, Muluk SC, Finol EA (2013) The importance of patient-specific regionally varying wall thickness in abdominal aortic aneurysm biomechanics. J Biomech Eng 135:81010
29. Schurink GW, van Baalen JM, Visser MJ, van Bockel JH (2000) Thrombus within an aortic aneurysm does not reduce pressure on the aneurysmal wall. J Vasc Surg 31:501–506
30. Sonesson B, Hansen F, Lanne T (1997) Abdominal aortic aneurysm: a general defect in the vasculature with focal manifestations in the abdominal aorta? J Vasc Surg 26:247–254
31. Speelman L, Schurink GW, Bosboom EM, Buth J, Breeuwer M, van de Vosse FN, Jacobs MH (2010) The mechanical role of thrombus on the growth rate of an abdominal aortic aneurysm. J Vasc Surg 51:19–26
32. Taubin G (1995) Curve and surface smoothing without shrinkage. In: IEEE Computer Society proceedings of the fifth international conference on computer vision (ICCV '95), p 852
33. Thubrikar MJ, Robicsek F, Labrosse M, Chervenkoff V, Fowler BL (2003) Effect of thrombus on abdominal aortic aneurysm wall dilation and stress. J Cardiovasc Surg (Torino) 44:67–77
34. van't Veer M, Buth J, Merkx M, Tonino P, van den Bosch H, Pijls N, van de Vosse F (2008) Biomechanical properties of abdominal

aortic aneurysms assessed by simultaneously measured pressure and volume changes in humans. J Vasc Surg 48:1401–1407
35. van Dam EA, Dams SD, Peters GW, Rutten MC, Schurink GW, Buth J, van de Vosse FN (2008) Non-linear viscoelastic behavior of abdominal aortic aneurysm thrombus. Biomech Model Mechanobiol 7:127–137
36. Vavourakis V, Papaharilaou Y, Ekaterinaris JA (2011) Coupled fluid–structure interaction hemodynamics in a zero-pressure state corrected arterial geometry. J Biomech 44:2453–2460
37. Wang DH, Makaroun M, Webster MW, Vorp DA (2001) Mechanical properties and microstructure of intraluminal thrombus from abdominal aortic aneurysm. J Biomech Eng 123:536–539
38. Wang DH, Makaroun MS, Webster MW, Vorp DA (2002) Effect of intraluminal thrombus on wall stress in patient-specific models of abdominal aortic aneurysm. J Vasc Surg 36:598–604
39. Wilson JS, Virag L, Di Achille P, Karsaj I, Humphrey JD (2013) Biochemomechanics of intraluminal thrombus in abdominal aortic aneurysms. J Biomech Eng 135:021011
40. Wilson KA, Lee AJ, Lee AJ, Hoskins PR, Fowkes FG, Ruckley CV, Bradbury AW (2003) The relationship between aortic wall distensibility and rupture of infrarenal abdominal aortic aneurysm. J Vasc Surg 37:112–117
41. Xenos M, Alemu Y, Zamfir D, Einav S, Ricotta JJ, Labropoulos N, Tassiopoulos A, Bluestein D (2010) The effect of angulation in abdominal aortic aneurysms: fluid–structure interaction simulations of idealized geometries. Med Biol Eng Comput 48:1175–1190
42. Yushkevich PA, Piven J, Hazlett HC, Smith RG, Ho S, Gee JC, Gerig G (2006) User-guided 3d active contour segmentation of anatomical structures: significantly improved efficiency and reliability. Neuroimage 31:1116–1128